SEMARAK ILMU PUBLISHING

Journal of Advanced Research in Fluid Mechanics and Thermal Sciences

Journal homepage:
https://semarakilmu.com.my/journals/index.php/fluid_mechanics_thermal_sciences/index
ISSN: 2289-7879

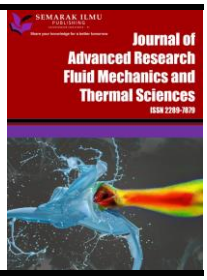

Homogeneous-Heterogeneous Reactions on Al_2O_3-Cu Hybrid Nanofluid Flow Over a Shrinking Sheet

Iskandar Waini[1,*], Farah Nadzirah Jamrus[2], Abdul Rahman Mohd Kasim[3,4], Anuar Ishak[5], Ioan Pop[6]

[1] Fakulti Teknologi Kejuruteraan Mekanikal dan Pembuatan, Universiti Teknikal Malaysia Melaka, 76100 Durian Tunggal, Malaysia
[2] Pengajian Sains Matematik, Kolej Pengajian Pengkomputeran, Informatik dan Media, Universiti Teknologi MARA (UiTM) Cawangan Melaka Kampus Bandaraya Melaka, 110 Off Jalan Hang Tuah, 75350 Melaka, Malaysia
[3] Centre for Mathematical Sciences, Universiti Malaysia Pahang, Gambang 26300, Malaysia
[4] Center for Research in Advanced Fluid and Process, University Malaysia Pahang, Lebuhraya Tun Razak, Gambang, Kuantan 26300, Pahang, Malaysia
[5] Department of Mathematical Sciences, Universiti Kebangsaan Malaysia, 43600 UKM Bangi, Malaysia
[6] Department of Mathematics, Babeş-Bolyai University, 400084 Cluj-Napoca, Romania

ARTICLE INFO

Article history:
Received 20 July 2022
Received in revised form 29 November 2022
Accepted 11 December 2022
Available online 30 December 2022

Keywords:
Fluid dynamics; heat transfer; similarity solutions; temporal stability

ABSTRACT

The effects of homogeneous-heterogeneous reaction on the fluid flow over a shrinking sheet is examined. A hybrid nanofluid is considered, with alumina and copper as the nanoparticles and water as the base liquid. The governing equations are solved numerically using similarity approach with the help of MATLAB software. Two outcomes are attained for several ranges of the mass flux parameter S. The friction factor as well as the concentration gradient enhances in the presence of nanoparticles, but the rate of heat transfer declines. Moreover, the concentration gradient is intensified for larger homogeneous and heterogeneous strength.

1. Introduction

The flow characteristics over a shrinking sheet was first discussed by Goldstein [1], while the stretching counterpart was established by Crane [2]. Wang [3] and Miklavčič and Wang [4] reported that the flow over a shrinking surface is possible by imposing certain suction strength on the surface. Similar observations were reported by several researchers [5-9]. According to them, the flow induced by a shrinking sheet shows physical phenomena quite distinct from the forward stretching flow.

The homogeneous (bulk) and heterogeneous (surface) reactions have significant applications in the biochemical, catalysis, and combustion systems. A simple of these reactions with equal and different diffusivities for autocatalyst and reactant in the boundary layer flow was introduced by Chaudhary and Merkin [10], respectively. Then, Merkin [11] extended the problem to the Blasius flow. Inspired by these studies, Kameswaran *et al.,* [12] considered the nanofluid flow over a

* *Corresponding author.*
E-mail address: iskandarwaini@utem.edu.my

https://doi.org/10.37934/arfmts.102.1.8597

stretching surface. They noticed that the fluid velocity was reduced, while the fluid concentration was increased in the presence of nanoparticles.

Also, they concluded that the concentration at the surface was declined for strong heterogeneous strength. Besides, Nandkeolyar *et al.,* [13] inspected the effect of heat generation and magnetic field. They discovered that the magnetic field reduces the species concentration as well as the nanofluid velocity. Meanwhile, the nanofluid temperature was increased caused by the heat generation. Moreover, Liu *et al.,* [14] considered the nanofluid flow past a stretching plate with four distinct shapes of Al_2O_3 nanoparticles. They discovered that the platelet nanoparticle gives the highest heat transfer capacity compared to others.

Choi and Eastman [15] used the term 'nanofluid', which refers to a mixture of the nanoparticles and the base fluid, which could increase its thermal conductivity. They expected that the addition of metallic nanoparticles in the base fluids can essentially improve the thermal conductivities of the conventional base fluids and enhance the heat transfer execution of these fluids. Then further studies reported that more advanced nanofluid could be engineered by mixing this nanofluid with another type of nanoparticles to form 'hybrid nanofluid'. This kind of fluid is believed to offer good thermal characteristics as compared to the base fluid and nanofluid containing single nanoparticles. Hybrid nanofluids are widely applied in many fields of heat transfer such as electronic cooling, generator cooling, coolant in machining, nuclear system cooling, transformer cooling, biomedical, drug reduction, refrigeration and etc. with better efficiency compared to nanofluids applicability. The experimental works involving the hybrid nanofluids were done [16,17]. On the other hand, the numerical studies on the hybrid nanofluids flow were done by Takabi and Salehi [18], Khashi'ie *et al.,* [19,20], Khan *et al.,* [21], Albeshri *et al.,* [22], Asghar and Ying [23], among others. Moreover, the dual solutions of the hybrid nanofluid flow were examined by Waini *et al.,* [24-26]. Recently, Yasir *et al.,* [27] reported the effect of copper and titania nanoparticles on a stretchable/shrinkable curved immersed in ethylene glycol. They concluded that, copper increases porosity and titania acts as a photocatalys. Additionally, the effect of SWCNTs-CuO/Ehylene glycol on a stagnation region of stretching/shrinking surface, while ZnO-MWCNTs/EO on Homann flow of hybrid nanofluid towards biaxial shrinking surface was reported by Yasir *et al.,* [28,29], respectively.

Motivated by the above-mentioned study, in the present paper, we study the effect of homogenous-heterogeneous reactions on hybrid (Al_2O_3-Cu/water) nanofluid flow over a stretching/shrinking sheet by considering the chemical reaction model as proposed by Chaudhary and Merkin [10] and Merkin [11]. In this analysis, we assume that the auto catalysis and reactant have the same diffusion coefficients. Different from the work reported by Ramesh *et al.,* [30], the present study considers both stretching and shrinking sheets, where multiple solutions are attained for the case of shrinking sheet and their temporal stabilities are determined is also one of the objectives of this investigation. By incorporating similarity transformations, the partial differential equations (PDE) of the flow model are converted to ordinary differential equations (ODE). These ODE are solved numerically by using rigorous MATLAB built-in solver bvp4c. Instead of analyzing the critical values of the physical parameters, their physical effects on the flow characteristics are also examined. Thus, it provides valuable information on the gradients of essential factors to control the boundary layer flow pattern. Then, the findings are then presented and discussed numerically and graphically where it will answer the research question of how the chemical reaction affect the fluid flow. The output obtained from this study will give insight to the research of catalysis which involve the chemical reaction where the study is done using the mathematical approach and embedded with theory of fluid flow. The results would benefit scientists and engineers to become familiar with the flow behaviour of nanofluids and the way to predict the properties of this fluid for possibility of using it in various engineering and industrial processes, such as, blood flows, lubrication processes with

grease and heavy oils, glass blowing, electronic chips, food stuff, slurries, etc. In addition, it should be stated that the results of the paper are new and original with many practical applications of nanofluids in the modern industry.

2. Methodology

The flow triggered by a shrinking sheet with alumina and copper hybrid nanoparticles is considered. The surface velocity is $u_w(x) = cx$ with constant c and the mass flux velocity is v_w. Meanwhile, the ambient and the surface temperatures are denoted by T_∞ and T_w, respectively, and both are constants. The homogeneous-heterogeneous reactions are also taking into consideration. Following Chaudhary and Merkin [10] and Merkin [11], a simple homogeneous reaction and the first order of heterogeneous reaction can be written as follows:

$$A + 2B \rightarrow 3B, \text{rates} = k_1 ab^2 \tag{1}$$

$$A \rightarrow B, \text{rates} = k_s a \tag{2}$$

where these processes are assumed to be isothermal. Here, a and b are the chemical concentrations for species A and B, respectively, with the rate constants k_1 and k_s. It is worth to mention the governing equation respected to the propose problem has been undergone the boundary layer approximations. Accordingly, the hybrid nanofluid equations are [11,13,30]:

$$\frac{\partial u}{\partial x} + \frac{\partial v}{\partial y} = 0 \tag{3}$$

$$u\frac{\partial u}{\partial x} + v\frac{\partial u}{\partial y} = \frac{\mu_{hnf}}{\rho_{hnf}}\frac{\partial^2 u}{\partial y^2} \tag{4}$$

$$u\frac{\partial T}{\partial x} + v\frac{\partial T}{\partial y} = \frac{k_{hnf}}{(\rho C_p)_{hnf}}\frac{\partial^2 T}{\partial y^2} \tag{5}$$

$$u\frac{\partial a}{\partial x} + v\frac{\partial a}{\partial y} = D_A\frac{\partial^2 a}{\partial y^2} - k_1 ab^2 \tag{6}$$

$$u\frac{\partial b}{\partial x} + v\frac{\partial b}{\partial y} = D_B\frac{\partial^2 b}{\partial y^2} + k_1 ab^2 \tag{7}$$

subject to

$$\begin{aligned} &v = v_w, u = u_w(x)\lambda, T = T_w, D_A\frac{\partial a}{\partial y} = k_s a, D_B\frac{\partial b}{\partial y} = -k_s a \text{ at } y = 0 \\ &u \rightarrow 0, T \rightarrow T_\infty, a \rightarrow a_0, b \rightarrow 0 \quad \text{as} \quad y \rightarrow \infty \end{aligned} \tag{8}$$

where the coordinates (x, y) with corresponding velocities (u, v) are measured along the x- *and* y-axes, while T represents the temperature. Besides, D_A and D_B are the corresponding diffusion coefficients of species A and B, and $a_0 > 0$. The thermophysical properties are given in Table 1 and Table 2. Note that φ_1 (Al_2O_3) and φ_2 (Cu) are the nanoparticles volume fractions where $\varphi_{hnf} = \varphi_1 + \varphi_2$, and the subscripts $n1$ and $n2$ correspond to their solid components. Further, the subscripts hnf and f respectively denote the hybrid nanofluid and the base fluid.

Table 1
Thermophysical properties of nanoparticles and water [31]

Properties	Base fluid water	Nanoparticles Cu	Al_2O_3
$\rho\ (kg/m^3)$	997.1	8933	3970
$C_p\ (J/kgK)$	4179	385	765
$k\ (W/mK)$	0.613	400	40
Prandtl number, Pr	6.2		

Table 2
Thermophysical properties of hybrid nanofluid [18]

Properties	Correlations
Thermal conductivity	$\frac{k_{hnf}}{k_f} = \frac{\frac{\varphi_1 k_{n1} + \varphi_2 k_{n2}}{\varphi_{hnf}} + 2k_f + 2(\varphi_1 k_{n1} + \varphi_2 k_{n2}) - 2\varphi_{hnf} k_f}{\frac{\varphi_1 k_{n1} + \varphi_2 k_{n2}}{\varphi_{hnf}} + 2k_f - (\varphi_1 k_{n1} + \varphi_2 k_{n2}) + \varphi_{hnf} k_f}$
Heat capacity	$(\rho C_p)_{hnf} = (1-\varphi_{hnf})(\rho C_p)_f + \varphi_1(\rho C_p)_{n1} + \varphi_2(\rho C_p)_{n2}$
Density	$\rho_{hnf} = (1-\varphi_{hnf})\rho_f + \varphi_1\rho_{n1} + \varphi_2\rho_{n2}$
Dynamic viscosity	$\mu_{hnf} = \frac{\mu_f}{(1-\varphi_{hnf})^{2.5}}$

To get similarity solution, the following variables are introduced [13,30]

$$\psi = \sqrt{c\nu_f}\, x f(\eta), \quad \eta = y\sqrt{c/\nu_f}, \quad \theta(\eta) = (T - T_\infty)/(T_w - T_\infty), \\ a = a_0 g(\eta), \quad b = a_0 h(\eta) \tag{9}$$

with ψ as the stream function where $u = \partial\psi/\partial y$ and $v = -\partial\psi/\partial x$, which yield

$$u = cx f'(\eta), \quad v = -\sqrt{c\nu_f}\, f(\eta) \tag{10}$$

The dimensionless variables in Eq. (9) are adopted from the previous studies [13,30]. The dimensionless variable η is defined as $\eta = y/\delta(x)$, where $\delta(x)$ is the boundary layer thickness. By implementing the order of magnitude analysis, one obtains $\delta(x) = \left(\nu_f x/u_w\right)^{1/2}$, which then implies

$$\eta = y\left(\frac{c}{\nu_f}\right)^{1/2}$$

where $u_w(x) = cx$. The dimensionless velocity is defined as $g(\eta) = u/u_w$ or $u = u_w g(\eta)$, with

$$u = \frac{\partial\psi}{\partial y} = \frac{\partial\psi}{\partial\eta}\frac{\partial\eta}{\partial y},$$

which then yields

$$\frac{\partial\psi}{\partial\eta} = x\left(c\nu_f\right)^{1/2} g(\eta).$$

Integrating both sides with respect to η gives

$$\psi = x\left(c\nu_f\right)^{1/2} f(\eta)$$

where $f'(\eta) = g(\eta)$.

Similar as velocity u which is expressed in terms of dimensionless quantity, $u/u_w = f'(\eta)$, the temperature T is also expressed in terms of dimensionless quantity as

$$\theta = \frac{T - T_\infty}{T_w - T_\infty}$$

which is unity at the wall, $\theta(0) = 1$, and zero far away from the wall, $\theta(\infty) = 0$. For further reading, one can refer to Avramenko *et al.,* [32], Avramenko and Shevchuk [33], and Waini *et al.,* [34].

The continuity Eq. (3) is identically satisfied. Now, Eq. (4) to Eq. (7) reduce to

$$\frac{\mu_{hnf}/\mu_f}{\rho_{hnf}/\rho_f} f''' + ff'' - f'^2 = 0 \tag{11}$$

$$\frac{1}{Pr} \frac{k_{hnf}/k_f}{(\rho C_p)_{hnf}/(\rho C_p)_f} \theta'' + f\theta' = 0 \tag{12}$$

$$\frac{1}{Sc} g'' + fg' - Kgh^2 = 0 \tag{13}$$

$$\frac{\delta}{Sc} h'' + fh' + Kgh^2 = 0 \tag{14}$$

subject to

$$\begin{aligned} &f(0) = S, \quad f'(0) = \lambda, \quad \theta(0) = 1, \quad g'(0) = K_s g(0), \quad \delta h'(0) = K_s g(0) \\ &f'(\eta) \to 0, \quad \theta(\eta) \to 0, \quad g(\eta) \to 1, \quad h(\eta) \to 0 \quad as \quad \eta \to \infty \end{aligned} \tag{15}$$

where primes indicate differentiation w.r.t. η. The physical parameters appear in Eq. (12) to Eq. (15) is the Prandtl number Pr, the Schmidt number Sc, the ratio of the diffusion coefficients δ, the strength of the homogeneous K and the heterogeneous K_s reactions, and the constant mass flux parameter S, defined as

$$Pr = \frac{(\mu C_p)_f}{k_f}, \quad Sc = \frac{\nu_f}{D_A}, \quad \delta = \frac{D_B}{D_A}, \quad K = \frac{k_1 a_0^2}{c}, \quad K_s = \frac{k_s}{D_A\sqrt{c/\nu_f}}, \quad S = -\frac{v_w}{\sqrt{c\nu_f}} \tag{16}$$

Here, $S < 0$ and $S > 0$ are for injection and suction cases, respectively, while $S = 0$ represents an impermeable case. Besides, $\lambda < 0$ and $\lambda > 0$ respectively represent the shrinking and stretching surfaces, while $\lambda = 0$ denotes a fixed surface. As discussed by Chaudhary and Merkin [10], both diffusion coefficients *(D_A* and *D_B)* are of comparable sizes, thus, these coefficients are assumed to be equal by taking $\delta = 1$. Hence, one gets

$$g(\eta) + h(\eta) = 1 \tag{17}$$

Using Eq. (17), Eq. (13) and Eq. (14) become

$$\frac{1}{Sc}g'' + fg' - Kg(1-g)^2 = 0 \tag{18}$$

subject to

$$g'(0) = K_s g(0), \quad g(\eta) \to 1 \quad as \quad \eta \to \infty \tag{19}$$

The skin friction coefficient C_f and the local Nusselt number Nu_x are defined as

$$C_f = \frac{\mu_{hnf}}{\rho_f u_w^2}\left(\frac{\partial u}{\partial y}\right)_{y=0}, \quad Nu_x = -\frac{xk_{hnf}}{k_f(T_w - T_\infty)}\left(\frac{\partial T}{\partial y}\right)_{y=0} \tag{20}$$

which then yield

$$Re_x^{1/2} C_f = \frac{\mu_{hnf}}{\mu_f} f''(0), \quad Re_x^{-1/2} Nu_x = -\frac{k_{hnf}}{k_f}\theta'(0) \tag{21}$$

where $Re_x = u_w x/\nu_f$ represents the local Reynolds number. Note that, when $\varphi_{hnf} = 0$ (regular fluid) for the permeable shrinking sheet, Eq. (11) has the exact solution [9,35]

$$f(\eta) = S - \frac{2}{S \pm \sqrt{S^2-4}}\left(1 - e^{-\frac{S \pm \sqrt{S^2-4}}{2}\eta}\right) \tag{22}$$

Then,

$$f''(0) = \frac{S \pm \sqrt{S^2-4}}{2} \tag{23}$$

Consequently, the present results can be compared with the exact solution (23) for validation purposes.

3. Temporal Stability Analysis

This stability analysis was employed by Merkin [36] and then popularized by Weidman *et al.,* [37]. To begin, first consider the following variables

$$\begin{gathered}\psi = \sqrt{c\nu_f}\, x f(\eta,\tau), \quad \eta = y\sqrt{c/\nu_f}, \quad \theta(\eta,\tau) = (T - T_\infty)/(T_w - T_\infty), \\ a = a_0 g(\eta,\tau), \quad b = a_0 h(\eta,\tau), \quad \tau = ct\end{gathered} \tag{24}$$

Now, the unsteady form of Eq. (4) to Eq. (7) are employed, while Eq. (3) remains unchanged. On using (24), one obtains

$$\frac{\mu_{hnf}/\mu_f}{\rho_{hnf}/\rho_f}\frac{\partial^3 f}{\partial \eta^3} + f\frac{\partial^2 f}{\partial \eta^2} - \left(\frac{\partial f}{\partial \eta}\right)^2 - \frac{\partial^2 f}{\partial \eta \partial \tau} = 0 \tag{25}$$

$$\frac{1}{Pr}\frac{k_{hnf}/k_f}{(\rho C_p)_{hnf}/(\rho C_p)_f}\frac{\partial^2\theta}{\partial\eta^2}+f\frac{\partial\theta}{\partial\eta}-\frac{\partial\theta}{\partial\tau}=0 \tag{26}$$

$$\frac{1}{Sc}\frac{\partial^2 g}{\partial\eta^2}+f\frac{\partial g}{\partial\eta}-Kg(1-g)^2-\frac{\partial g}{\partial\tau}=0 \tag{27}$$

subject to

$$\begin{aligned} &f(0,\tau)=S,\quad f'(0,\tau)=\lambda,\quad \theta(0,\tau)=1,\quad g'(0,\tau)=K_s g(0,\tau)\\ &f'(\eta,\tau)\to 0,\quad \theta(\eta,\tau)\to 0,\quad g(\eta,\tau)\to 1\quad as\quad \eta\to\infty \end{aligned} \tag{28}$$

Then, the disturbance is applied to the steady solution $f=f_0(\eta)$, $\theta=\theta_0(\eta)$, and $g=g_0(\eta)$ of Eq. (11), Eq. (12) and Eq. (18) by employing the following relations [37]

$$\begin{aligned} &f(\eta,\tau)=f_0(\eta)+e^{-\gamma\tau}F(\eta),\quad \theta(\eta,\tau)=\theta_0(\eta)+e^{-\gamma\tau}H(\eta),\\ &g(\eta,\tau)=g_0(\eta)+e^{-\gamma\tau}G(\eta) \end{aligned} \tag{29}$$

The eigenvalue γ will determine the stability of the solutions as $\tau\to\infty$. Also, $F(\eta)$, $H(\eta)$, and $G(\eta)$ are relatively small compared to $f_0(\eta)$, $\theta_0(\eta)$, and $g_0(\eta)$. By employing Eq. (29), and after linearization, Eq. (25) to Eq. (27) become

$$\frac{\mu_{hnf}/\mu_f}{\rho_{hnf}/\rho_f}F'''+f_0F''+f_0''F-2f_0'F'+\gamma F'=0 \tag{30}$$

$$\frac{1}{Pr}\frac{k_{hnf}/k_f}{(\rho C_p)_{hnf}/(\rho C_p)_f}H''+f_0H'+\theta_0'F+\gamma H=0 \tag{31}$$

$$\frac{1}{Sc}G''+f_0G'+g_0'F-K(1-4g_0+3g_0^2)G+\gamma G=0 \tag{32}$$

subject to

$$\begin{aligned} &F(0)=0,\quad F'(0)=0,\quad H(0)=0,\quad G'(0)=K_sG(0)\\ &F'(\eta)\to 0,\quad H(\eta)\to 0,\quad G(\eta)\to 0\quad as\quad \eta\to\infty \end{aligned} \tag{33}$$

To obtain γ from Eq. (30) to Eq. (32), the new boundary condition $F''(0)=1$ is included in Eq. (33) to replace $F'(\eta)\to 0\ as\ \eta\to\infty$ [38].

4. Results and Discussion

By utilising the package bvp4c in MATLAB software, Eq. (11), Eq. (12), and Eq. (18) subject to Eq. (15) and Eq. (19) are numerically solved. This method employs the 3-stage Lobatto IIIa formula [39].

The values of $f''(0)$ for various of S when $\varphi_{hnf}=0$ and $\lambda=-1$ are compared with the exact solution (23) and Yasin *et al.,* [9]. It is found that the results are comparable for each S considered, as shown in Table 3. Also, Table 4 shows the comparison of $f''(0)$ and $-\theta'(0)$ with Hamad [40] with different values of φ_1 when $S=0$, $\lambda=1$, and $\mathrm{Pr}=6.2$ for Al_2O_3/water ($\varphi_2=0$). We notice that the present results are comparable with that mentioned literature. Next, Table 5 displays the values of the skin friction coefficient $Re_x^{1/2}\,C_f$, local Nusselt number $Re_x^{-1/2}Nu_x$ and the concentration

gradient $g'(0)$ with various parameters when $S = 0, \lambda = 1$ (stretching sheet), $\mathrm{Sc} = 1$, and $\mathrm{Pr} = 6.2$. The rising of φ_{hnf} tends to upsurge the rates of $Re_x^{-1/2} Nu_x$, but reduce the rates of $Re_x^{1/2}\, C_f$ and $g'(0)$. Besides, the rise of K declines the values of $g'(0)$, whereas the effect of larger K_s is to enhance the values of $g'(0)$. However, the values of $Re_x^{1/2}\, C_f$ and $Re_x^{-1/2} Nu_x$ are not affected by these parameters.

Table 3
Values of $f''(0)$ for various S when $\varphi_{hnf} = 0$ and $\lambda = -1$

S	Exact solution Eq. (23)	Yasin *et al.,* [9]	Present results
2	1	1.0000	1.00000
3	2.61803 (0.38197)	2.6180 (0.3820)	2.61803 (0.38197)
4	3.73205 (0.26795)	3.7321 (0.2680)	3.73205 (0.26795)

Results in "( )" are the second solutions

Table 4
Values of $f''(0)$ and $-\theta'(0)$ when $\mathrm{Pr} = 6.2, S = \varphi_2 = 0$ and $\lambda = 1$ for different values of φ_1 (Al_2O_3/water)

φ_1	Hamad *et al.,* [40]		Present results	
	$f''(0)$	$-\theta'(0)$	$f''(0)$	$-\theta'(0)$
0.05	-1.00538	1.62246	-1.00538	1.62246
0.1	-0.99877	1.49170	-0.99877	1.49170
0.15	-0.98185	1.37543	-0.98184	1.37543
0.2	-0.95592	1.27118	-0.95592	1.27118

Table 5
Values of $Re_x^{1/2}\, C_f$, $Re_x^{-1/2} Nu_x$ and $g'(0)$ with various parameters when $S = 0, \lambda = 1$ (stretching sheet), $Sc = 1$, and $\mathrm{Pr} = 6.2$

φ_{hnf}	K	K_s	$Re_x^{1/2}\, C_f$	$Re_x^{-1/2} Nu_x$	$g'(0)$
2%	1	1	-1.08022	1.80634	0.25144
4%			-1.16179	1.84203	0.24593
6%			-1.24516	1.87812	0.24137
2%	0.5		-1.08022	1.80634	0.31966
	1.5		-1.08022	1.80634	0.13871
	1.8		-1.08022	1.80634	0.01205
	1	2	-1.08022	1.80634	0.29717
		4	-1.08022	1.80634	0.33351
		6	-1.08022	1.80634	0.34923

Figure 1 to Figure 3 show the variations of $Re_x^{1/2} C_f$, $Re_x^{-1/2} Nu_x$ and $g'(0)$ against S for various φ_{hnf} when $\lambda = -1, \mathrm{Pr} = 6.2, \mathrm{Sc} = 1$, and $K = K_s = 0.5$. These figures show that the values of $Re_x^{1/2} C_f$ and $g'(0)$ are intensified, whereas the values of $Re_x^{-1/2} Nu_x$ are reduced with the rise of φ_{hnf}. Besides, for fixed values of the selected parameters, it is observed that the dual solutions are possible for some range of suction strength S. The critical values are $S_c = 1.9474, 1.9065, 1.8750$ for $\varphi_{hnf} = 2\%, 4\%, 6\%$, respectively. This observation is consistent with the fact that the flow over a shrinking surface is only possible by imposing an appropriate suction strength on the surface as discussed by Miklavčič and Wang [4]. Also, these figures expose that the boundary layer separates slower for larger φ_{hnf}. Moreover, the variations of $g'(0)$ against S for different values of K and K_s when $\lambda = -1, \mathrm{Pr} = 6.2, \mathrm{Sc} = 1$ and $\varphi_{hnf} = 2\%$ are presented in Figure 4 and Figure 5. The values of $g'(0)$ are upsurged for larger values of K and the increment is more pronounced with the rise of K_s.

The critical values occur at $S_c = 1.9474$ for all selected values of K and K_s. Further, the effect of K and K_s on $g(\eta)$ when $\lambda = -1, S = 2, \mathrm{Pr} = 6.2, \mathrm{Sc} = 1$ and $\varphi_{hnf} = 2\%$ are depicted in Figure 6 and Figure 7. The decreasing pattern on both branch solutions of $g(\eta)$ is noticed for larger values of K and K_s.

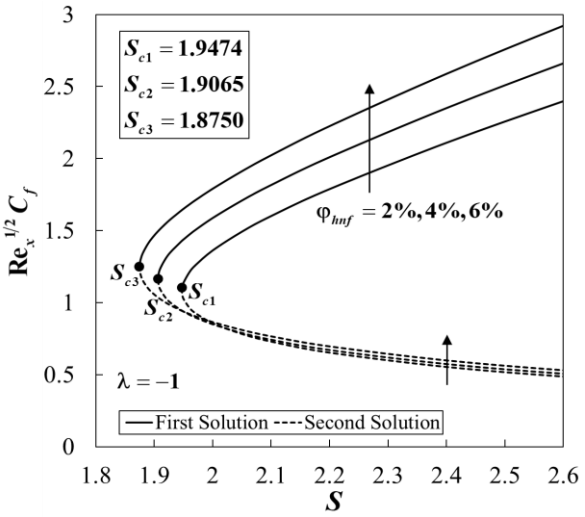

Fig. 1. $Re_x^{1/2} C_f$ vs S and φ_{hnf}

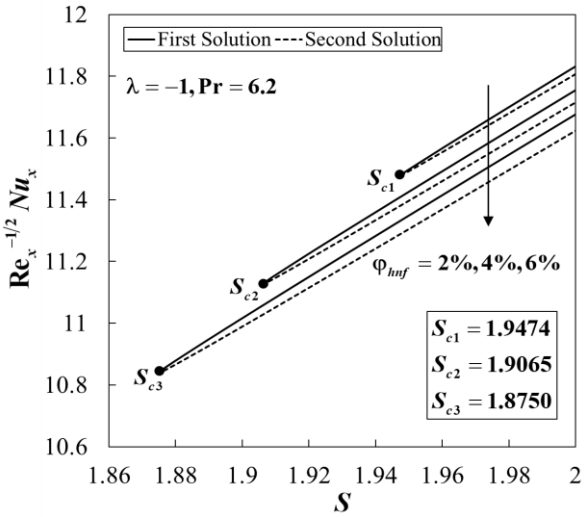

Fig. 2. $Re_x^{-1/2} Nu_x$ vs S and φ_{hnf}

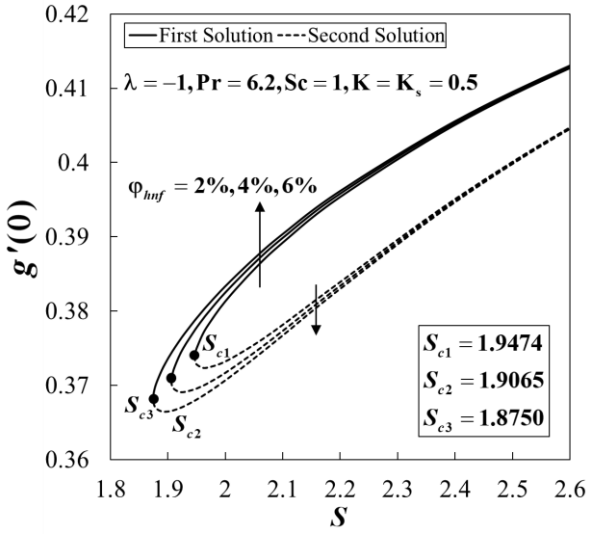

Fig. 3. $g'(0)$ vs S and φ_{hnf}

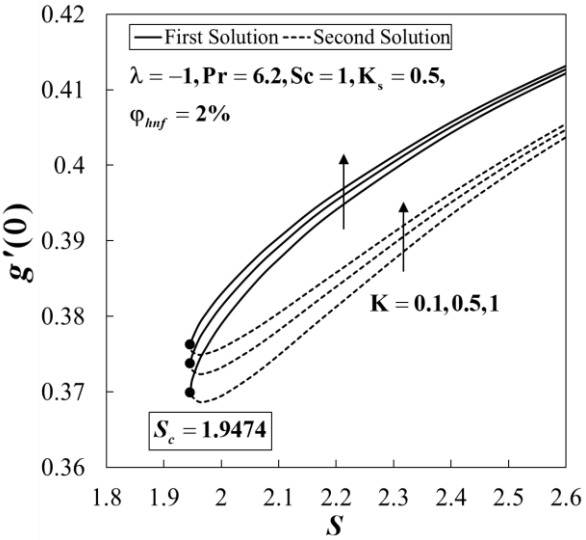

Fig. 4. $g'(0)$ vs S and K

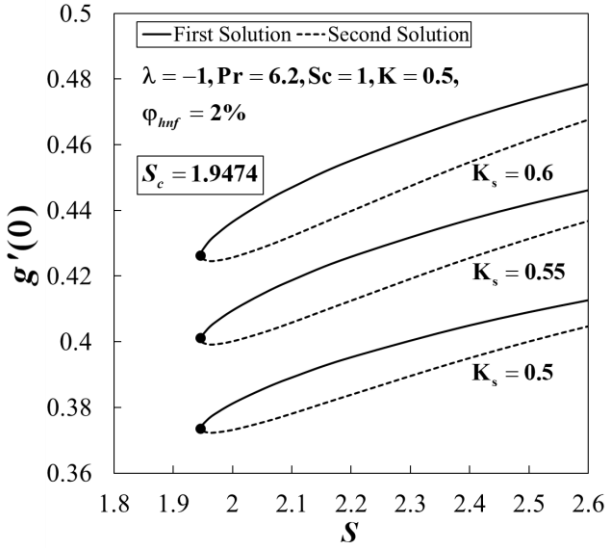

Fig. 5. $g'(0)$ vs S and K_S

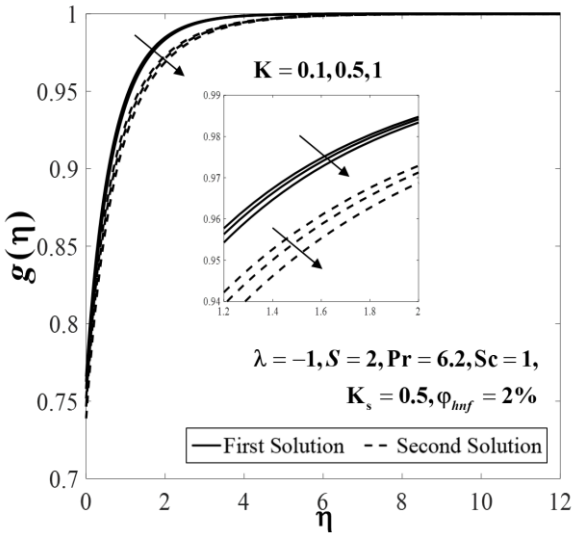

Fig. 6. $g(\eta)$ with K

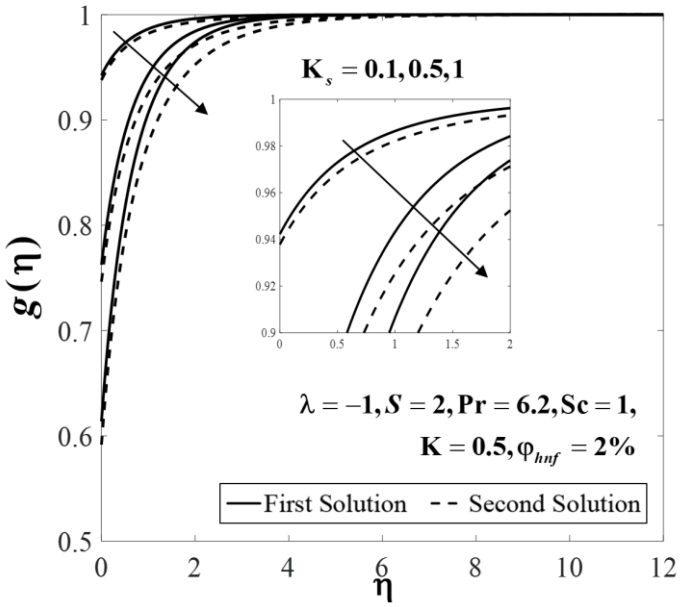

Fig. 7. $g(\eta)$ with K_S

Moreover, the variations of γ against S when $\lambda = -1$, and $\varphi_{hnf} = 2\%$ is portrayed in Figure 8. For positive eigenvalues γ, it is seen that $e^{-\gamma\tau} \to 0$ as $\tau \to \infty$. In contrast, for negative values of γ, it is found that $e^{-\gamma\tau} \to \infty$. These observations indicate that the first solution is stable over time, while the second solution is unstable and thus not physically reliable in the long run.

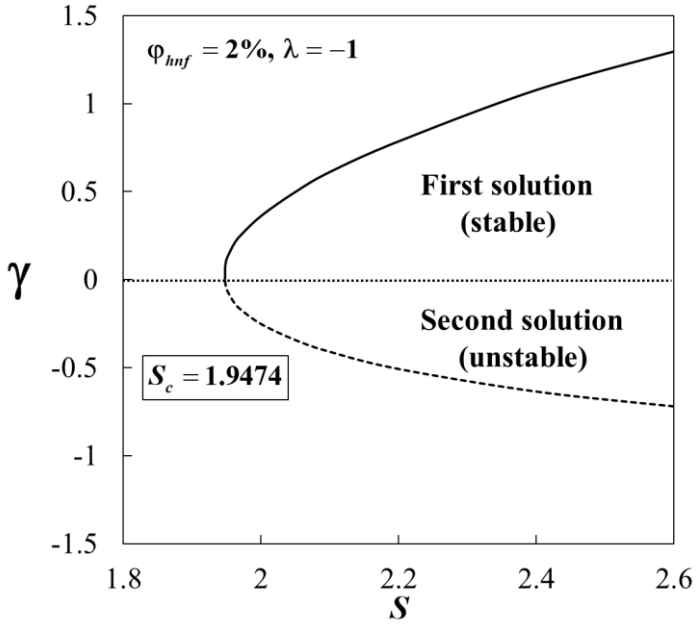

Fig. 8. γ against S

5. Conclusions

The effects of Al_2O_3-Cu hybrid nanoparticles on the flow over a shrinking sheet was accomplished. Both homogeneous and heterogeneous reaction effects were considered. Findings found that dual solutions exist for certain parameters. It was found that the critical values occur in the suction region $(S > 0)$. The increment of $Re_x^{1/2} C_f$ and $g'(0)$, while the reduction of $Re_x^{-1/2} Nu_x$ were observed with the rise of φ_{hnf}. Also, the values of $g'(0)$ increased for larger values of K and K_s. Finally, it was discovered that the first solution is stable over time, whereas the second is not.

Acknowledgement

The authors gratefully acknowledge Universiti Teknikal Malaysia Melaka (PJP/2022/FTKMP/S01891) and Universiti Kebangsaan Malaysia for the financial support. Appreciation also goes to Universiti Malaysia Pahang under RDU223015.

References

[1] Goldstein, Sydney. "On backward boundary layers and flow in converging passages." *Journal of Fluid Mechanics* 21, no. 1 (1965): 33-45. https://doi.org/10.1017/S0022112065000034

[2] Crane, Lawrence J. "Flow past a stretching plate." *Zeitschrift für angewandte Mathematik und Physik ZAMP* 21 (1970): 645-647. https://doi.org/10.1007/BF01587695

[3] Wang, C. Y. "Liquid film on an unsteady stretching surface." *Quarterly of Applied Mathematics* 48, no. 4 (1990): 601-610. https://doi.org/10.1090/qam/1079908

[4] Miklavčič, M., and C. Wang. "Viscous flow due to a shrinking sheet." *Quarterly of Applied Mathematics* 64, no. 2 (2006): 283-290. https://doi.org/10.1090/S0033-569X-06-01002-5

[5] Fang, Tiegang. "Boundary layer flow over a shrinking sheet with power-law velocity." *International Journal of Heat and Mass Transfer* 51, no. 25-26 (2008): 5838-5843. https://doi.org/10.1016/j.ijheatmasstransfer.2008.04.067

[6] Fang, Tiegang, Shanshan Yao, Ji Zhang, and Abdul Aziz. "Viscous flow over a shrinking sheet with a second order slip flow model." *Communications in Nonlinear Science and Numerical Simulation* 15, no. 7 (2010): 1831-1842. https://doi.org/10.1016/j.cnsns.2009.07.017

[7] Yacob, Nor Azizah, and Anuar Ishak. "Micropolar fluid flow over a shrinking sheet." *Meccanica* 47 (2012): 293-299. https://doi.org/10.1007/s11012-011-9439-8

[8] Roşca, Alin V., and Ioan Pop. "Flow and heat transfer over a vertical permeable stretching/shrinking sheet with a second order slip." *International Journal of Heat and Mass Transfer* 60 (2013): 355-364. https://doi.org/10.1016/j.ijheatmasstransfer.2012.12.028

[9] Yasin, Mohd Hafizi Mat, Anuar Ishak, and Ioan Pop. "Boundary layer flow and heat transfer past a permeable shrinking surface embedded in a porous medium with a second-order slip: A stability analysis." *Applied Thermal Engineering* 115 (2017): 1407-1411. https://doi.org/10.1016/j.applthermaleng.2016.08.080

[10] Chaudhary, M. A., and J. H. Merkin. "A simple isothermal model for homogeneous-heterogeneous reactions in boundary-layer flow. I Equal diffusivities." *Fluid Dynamics Research* 16, no. 6 (1995): 311-333. https://doi.org/10.1016/0169-5983(95)00015-6

[11] Merkin, J. H. "A model for isothermal homogeneous-heterogeneous reactions in boundary-layer flow." *Mathematical and Computer Modelling* 24, no. 8 (1996): 125-136. https://doi.org/10.1016/0895-7177(96)00145-8

[12] Kameswaran, P. K., S. Shaw, P. V. S. N. Sibanda, and P. V. S. N. Murthy. "Homogeneous-heterogeneous reactions in a nanofluid flow due to a porous stretching sheet." *International Journal of Heat and Mass Transfer* 57, no. 2 (2013): 465-472. https://doi.org/10.1016/j.ijheatmasstransfer.2012.10.047

[13] Nandkeolyar, Raj, Peri K. Kameswaran, Sachin Shaw, and Precious Sibanda. "Heat transfer on nanofluid flow with homogeneous-heterogeneous reactions and internal heat generation." *Journal of Heat Transfer* 136, no. 12 (2014): 122001. https://doi.org/10.1115/1.4028644

[14] Liu, Chunyan, Mingyang Pan, Liancun Zheng, and Ping Lin. "Effects of heterogeneous catalysis in porous media on nanofluid-based reactions." *International Communications in Heat and Mass Transfer* 110 (2020): 104434. https://doi.org/10.1016/j.icheatmasstransfer.2019.104434

[15] Choi, S. US, and Jeffrey A. Eastman. *Enhancing thermal conductivity of fluids with nanoparticles.* No. ANL/MSD/CP-84938; CONF-951135-29. Argonne National Lab.(ANL), Argonne, IL (United States), 1995.

[16] Jana, Soumen, Amin Salehi-Khojin, and Wei-Hong Zhong. "Enhancement of fluid thermal conductivity by the addition of single and hybrid nano-additives." *Thermochimica Acta* 462, no. 1-2 (2007): 45-55. https://doi.org/10.1016/j.tca.2007.06.009

[17] Suresh, S., K. P. Venkitaraj, P. Selvakumar, and M. Chandrasekar. "Synthesis of Al_2O_3-Cu/water hybrid nanofluids using two step method and its thermo physical properties." *Colloids and Surfaces A: Physicochemical and Engineering Aspects* 388, no. 1-3 (2011): 41-48. https://doi.org/10.1016/j.colsurfa.2011.08.005

[18] Takabi, Behrouz, and Saeed Salehi. "Augmentation of the heat transfer performance of a sinusoidal corrugated enclosure by employing hybrid nanofluid." *Advances in Mechanical Engineering* 6 (2014): 147059. https://doi.org/10.1155/2014/147059

[19] Khashi'ie, Najiyah Safwa, Iskandar Waini, Syazwani Mohd Zokri, Abdul Rahman Mohd Kasim, Norihan Md Arifin, and Ioan Pop. "Stagnation point flow of a second-grade hybrid nanofluid induced by a Riga plate." *International Journal of Numerical Methods for Heat & Fluid Flow* 32, no. 7 (2021): 2221-2239. https://doi.org/10.1108/HFF-08-2021-0534

[20] Khashi'ie, Najiyah Safwa, Ezad Hafidz Hafidzuddin, Norihan Md Arifin, and Nadihah Wahi. "Stagnation point flow of hybrid nanofluid over a permeable vertical stretching/shrinking cylinder with thermal stratification effect." *CFD Letters* 12, no. 2 (2020): 80-94.

[21] Khan, Umair, Aurang Zaib, Anuar Ishak, El-Sayed M. Sherif, Iskandar Waini, Yu-Ming Chu, and Ioan Pop. "Radiative mixed convective flow induced by hybrid nanofluid over a porous vertical cylinder in a porous media with irregular heat sink/source." *Case Studies in Thermal Engineering* 30 (2022): 101711. https://doi.org/10.1016/j.csite.2021.101711

[22] Albeshri, Badr Ali Bzya, Nazrul Islam, Ahmad Yahya Bokhary, and Amjad Ali Pasha. "Hydrodynamic Analysis of Laminar Mixed Convective Flow of Ag-TiO_2-Water Hybrid Nanofluid in a Horizontal Annulus." *CFD Letters* 13, no. 7 (2021): 47-57. https://doi.org/10.37934/cfdl.13.7.4557

[23] Asghar, Adnan, and Teh Yuan Ying,. "Three dimensional MHD hybrid nanofluid Flow with rotating stretching/shrinking sheet and Joule heating." *CFD Letters* 13, no. 8 (2021): 1-19. https://doi.org/10.37934/cfdl.13.8.119

[24] Waini, Iskandar, Anuar Ishak, and Ioan Pop. "Melting heat transfer of a hybrid nanofluid flow towards a stagnation point region with second-order slip." *Proceedings of the Institution of Mechanical Engineers, Part E: Journal of Process Mechanical Engineering* 235, no. 2 (2021): 405-415. https://doi.org/10.1177/0954408920961213

[25] Waini, Iskandar, Anuar Ishak, and Ioan Pop. "Hybrid nanofluid flow over a permeable non-isothermal shrinking surface." *Mathematics* 9, no. 5 (2021): 538. https://doi.org/10.3390/math9050538

[26] Waini, Iskandar, Anuar Ishak, and Ioan Pop. "Unsteady hybrid nanofluid flow on a stagnation point of a permeable rigid surface." *ZAMM-Journal of Applied Mathematics and Mechanics/Zeitschrift für Angewandte Mathematik und Mechanik* 101, no. 6 (2021): e202000193. https://doi.org/10.1002/zamm.202000193

[27] Yasir, Muhammad, Masood Khan, Mahnoor Sarfraz, Dina Abuzaid, and Malik Zaka Ullah. "Exploration of the dynamics of ethylene glycol conveying copper and titania nanoparticles on a stretchable/shrinkable curved object: stability analysis." *International Communications in Heat and Mass Transfer* 137 (2022): 106225. https://doi.org/10.1016/j.icheatmasstransfer.2022.106225

[28] Yasir, Muhammad, Abdul Hafeez, and Masood Khan. "Thermal conductivity performance in hybrid (SWCNTs-CuO/Ehylene glycol) nanofluid flow: Dual solutions." *Ain Shams Engineering Journal* 13, no. 5 (2022): 101703. https://doi.org/10.1016/j.asej.2022.101703

[29] Yasir, Muhammad, Mahnoor Sarfraz, Masood Khan, Abdullah Khamis Alzahrani, and Malik Zaka Ullah. "Estimation of dual branch solutions for Homann flow of hybrid nanofluid towards biaxial shrinking surface." *Journal of Petroleum Science and Engineering* 218 (2022): 110990. https://doi.org/10.1016/j.petrol.2022.110990

[30] Ramesh, G. K., S. Manjunatha, and B. J. Gireesha. "Impact of homogeneous-heterogeneous reactions in a hybrid nanoliquid flow due to porous medium." *Heat Transfer-Asian Research* 48, no. 8 (2019): 3866-3884. https://doi.org/10.1002/htj.21572

[31] Oztop, Hakan F., and Eiyad Abu-Nada. "Numerical study of natural convection in partially heated rectangular enclosures filled with nanofluids." *International Journal of Heat and Fluid Flow* 29, no. 5 (2008): 1326-1336. https://doi.org/10.1016/j.ijheatfluidflow.2008.04.009

[32] Avramenko, A. A., S. G. Kobzar, I. V. Shevchuk, A. V. Kuznetsov, and L. T. Iwanisov. "Symmetry of turbulent boundary-layer flows: investigation of different eddy viscosity models." *Acta Mechanica* 151 (2001): 1-14. https://doi.org/10.1007/BF01272521

[33] Avramenko, A. A., and I. V. Shevchuk. "Lie group analysis and general forms of self-similar parabolic equations for fluid flow, heat and mass transfer of nanofluids." *Journal of Thermal Analysis and Calorimetry* 135 (2019): 223-235. https://doi.org/10.1007/s10973-018-7053-x

[34] Waini, Iskandar, A. Ishak, and Ioan Pop. "Flow over a shrinking sheet containing hybrid nanoparticles with nonlinear thermal radiation and magnetohydrodynamic effects." *Waves in Random and Complex Media* (2022): 1-19. https://doi.org/10.1080/17455030.2022.2091179

[35] Waini, Iskandar, Anuar Ishak, and Ioan Pop. "Flow and heat transfer along a permeable stretching/shrinking curved surface in a hybrid nanofluid." *Physica Scripta* 94, no. 10 (2019): 105219. https://doi.org/10.1088/1402-4896/ab0fd5

[36] Merkin, J. H. "On dual solutions occurring in mixed convection in a porous medium." *Journal of Engineering Mathematics* 20, no. 2 (1986): 171-179. https://doi.org/10.1007/BF00042775

[37] Weidman, P. D., D. G. Kubitschek, and A. M. J. Davis. "The effect of transpiration on self-similar boundary layer flow over moving surfaces." *International Journal of Engineering Science* 44, no. 11-12 (2006): 730-737. https://doi.org/10.1016/j.ijengsci.2006.04.005

[38] Harris, S. D., D. B. Ingham, and I. Pop. "Mixed convection boundary-layer flow near the stagnation point on a vertical surface in a porous medium: Brinkman model with slip." *Transport in Porous Media* 77 (2009): 267-285. https://doi.org/10.1007/s11242-008-9309-6

[39] Shampine, Lawrence F., Lawrence F. Shampine, Ian Gladwell, and S. Thompson. *Solving ODEs with matlab*. Cambridge University Press, 2003. https://doi.org/10.1017/CBO9780511615542

[40] Hamad, M. A. A. "Analytical solution of natural convection flow of a nanofluid over a linearly stretching sheet in the presence of magnetic field." *International Communications in Heat and Mass Transfer* 38, no. 4 (2011): 487-492. https://doi.org/10.1016/j.icheatmasstransfer.2010.12.042